Review Article | Neuroimaging and Head & Neck

http://dx.doi.org/10.3348/kjr.2015.16.3.550
pISSN 1229-6929 · eISSN 2005-8330
Korean J Radiol 2015;16(3):550-559

Korean Journal of Radiology
KJR

Physiological and Functional Magnetic Resonance Imaging Using Balanced Steady-state Free Precession

Sung-Hong Park, PhD[1], Paul Kyu Han, MS[1], Seung Hong Choi, MD[2]

[1]Magnetic Resonance Imaging Lab, Department of Bio and Brain Engineering, Korea Advanced Institute of Science and Technology, Daejeon 305-701, Korea; [2]Department of Radiology, Seoul National University College of Medicine, Seoul 110-744, Korea

Balanced steady-state free precession (bSSFP) is a highly efficient pulse sequence that is known to provide the highest signal-to-noise ratio per unit time. Recently, bSSFP is getting increasingly popular in both the research and clinical communities. This review will be focusing on the application of the bSSFP technique in the context of probing the physiological and functional information. In the first part of this review, the basic principles of bSSFP are briefly covered. Afterwards, recent developments related to the application of bSSFP, in terms of physiological and functional imaging, are introduced and reviewed. Despite its long development history, bSSFP is still a promising technique that has many potential benefits for obtaining high-resolution physiological and functional images.

Index terms: *bSSFP; TrueFISP; FIESTA; bFFE; Physiological MRI; Arterial spin labeling; fMRI*

INTRODUCTION

Magnetic resonance imaging (MRI) has considerably improved over the last 20 years because of its noninvasiveness, high soft tissue contrast, and availability of physiological, metabolic, and functional information beyond anatomical information. Physiological MRI without contrast agent has been typically performed with a dedicated magnetization preparation module followed by a fast data readout sequence. Functional MRI (fMRI) also requires a fast data readout scheme for high temporal resolution to capture hemodynamic responses associated with neuronal activities. Although many fast imaging techniques exist with MRI, echo planar imaging (EPI) has been the first choice as the data readout sequence for physiological MRI and fMRI because of its speed, sensitivity to the initial magnetization difference, and good T2* contrast (in case of fMRI). However, EPI suffers from distortion and signal degradation induced by magnetic field inhomogeneity or susceptibility effects, and it also is subjected to T2* blurring due to the acquisition of multiple K-space lines after a single radio frequency (RF) excitation. These factors limit the spatial resolution and image quality of the physiological MRI and fMRI with EPI. Other non-EPI based readout approaches, including rapid imaging with refocused echoes and gradient and spin echo, can be used to minimize susceptible artifacts (1-3), at the cost of either lower temporal resolution, blurring, or lower signal due to noise ratio per unit time.

Balanced steady-state free precession (bSSFP), is called true fast imaging with steady-state precession (Siemens Healthcare, Erlangen, Germany), fast imaging employing steady-state acquisition (FIESTA) (GE Healthcare,

Received April 7, 2014; accepted after revision February 5, 2015. This research was supported by the National Research Foundation of Korea (NRF-2013R1A1A1061759 and NRF-2013M3A9B2076548).
Corresponding author: Sung-Hong Park, PhD, Department of Bio and Brain Engineering, Korea Advanced Institute of Science and Technology, 291 Daehak-ro, Yuseong-gu, Daejeon 305-701, Korea.
• Tel: (8242) 350-7305 • Fax: (8242) 350-4310
• E-mail: sunghongpark@kaist.ac.kr

Korean Journal of Radiology
KJR

Buckinghamshire, United Kingdom), or balanced fast field echo (Philips Healthcare, Best, the Netherlands), and it is a kind of gradient recalled echo (GRE) sequence that allows for fast data acquisition. The bSSFP sequence utilizes single RF excitation per each K-space line, avoiding the problems associated with EPI. The bSSFP sequence has had a long history since its development. The first discovery of the technique dates back to the works of Carr (4) in 1958, and, since then, the technique has been continuously rediscovered (5) and refined (6). However, this technique has not, been readily used, until recently, in the research community, due to the complicated nature of the signal source and difficulty in obtaining a stable signal without the help of technical advancements in hardware specification. Compared to other GRE sequences, bSSFP provides higher signal to noise ratio (SNR) within a short scan time, frequently making this technique used for fast high-resolution anatomical imaging. The bSSFP sequence has higher sensitivity due to the initial magnetization differences (7) and also due to the subtle frequency changes, such as those induced by blood oxygenation level dependent (BOLD) effects (8). Based on this notion, bSSFP has been recently applied for distortion-free high-resolution physiological and functional MRI, in replacement of EPI, and it will be introduced, in detail, within this article. To fully utilize bSSFP for physiological and functional MRI, however, the unique signal characteristics of bSSFP should be appropriately understood (7, 9, 10).

In this article, the basic principles of bSSFP will be briefly reviewed, along with explanations regarding the unique signal characteristics of bSSFP. This paper will then focus on introducing the recent techniques and the important contemporary developments made in terms of the application of bSSFP for imaging physiological and functional information. The problems and potential applications of the physiological and functional imaging with bSSFP will be also discussed.

Basic Principles

Balanced steady-state free precession is a steady-state technique that utilizes residual transverse magnetization from previous RF excitations. While the time to repeat (TR) is much shorter than the T2 of an object, its transverse magnetization remains at the end of each TR before the next excitation. Unlike spoiled gradient echo sequences, this residual transverse magnetization is not removed in bSSFP. The transverse magnetization (along with the longitudinal magnetization) is used for the next RF excitation, providing the high signal in a very short TR (typically 3–6 ms). This action is achieved by a rapid, consecutive train of excitation pulses with "balanced" gradients (Fig. 1). The gradients are made to equally cancel out each of the three spatial directions (i.e., slice-selection, phase-encoding, and frequency-encoding directions) by the end of each TR and not to contribute to the accumulation of the magnetization phases. The signal phase is only dependent on the frequency shift (Δf) that is induced by magnetic field inhomogeneity, susceptibility, and chemical shifts, evolving in the amount of $2 \cdot \pi \cdot \Delta f \cdot TR$ during each TR.

Let's assume a spin is on resonance (i.e., $\Delta f = 0$) and TR < T2. When we apply for an initial RF excitation with a flip angle $\alpha/2$ and then a series of RF excitations with a flip angle sequence of $-\alpha, \alpha, -\alpha, \alpha, \ldots$, the magnetization initially flips toward the x-axis and then alternates between the +x and -x axes, allowing for high transverse magnetizations, in a balanced way, between consecutive RF excitations (Fig. 2). RF excitations at the same transmission phase will simply change the longitudinal and transverse magnetizations in an unbalanced way and, thus, cannot consistently provide high signals (corresponding to the dark bands in the bSSFP images). It should be noted that the negative flip angle ($-\alpha$) can be achieved by changing the transmission phase of the RF pulse by 180° (e.g.,

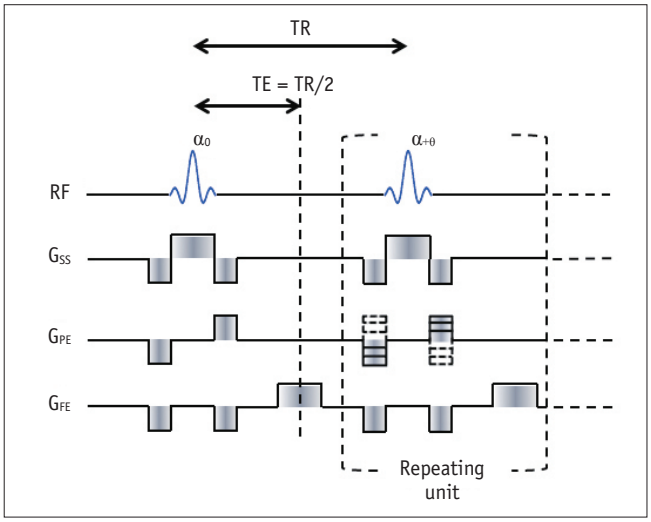

Fig. 1. Pulse sequence diagram of balanced steady-state free precession. Sum of all gradients in each of three directions (slice-selection, phase-encoding, and frequency-encoding) is zero. Phase of radio frequency (RF) pulse, denoted as phase-cycling angle (θ), can be incremented after every repetition time (TR). Echo time (TE) is typically set to half of TR. G_{SS}, G_{PE}, and G_{FE} represent gradients for slice selection, phase encoding, and frequency encoding, respectively.

applying the RF energy along the -y axis in contrast to the +y axis). Changing the transmission phases of the RF excitations is called "phase cycling". "Phase cycling angle" (ϕ_{cyc}) is defined as the increment of the transmission RF phase per TR. The flip angle sequence of -α, α, -α, α, ..., corresponds to the phase cycling angle of 180° because the transmission phase increases by 180° per TR.

On the other hand, if the phase evolution of a spin during each TR ($2\cdot\pi\cdot\Delta f\cdot TR$) happens to be 180° rather than 0° because of the frequency shift (Δf), the magnetization initially flips toward the +x axis and, then, automatically evolves to the -x axis during one TR, and, thus, a flip angle sequence of α, α, α, α, ..., (instead of -α, α, -α, α, ...) provides the balanced magnetizations, implying that the phase evolution per TR due to frequency shifts ($2\cdot\pi\cdot\Delta f\cdot TR$) and the phase cycling angle (ϕ_{cyc}) should be considered together and, ultimately, the sum of the two terms (ϕ_{tot}) should be close to 180° (i.e., $\phi_{tot} = \phi_{cyc} + 2\cdot\pi\cdot\Delta f\cdot TR \cong 180°$), in order for bSSFP to generate stable signals. In most clinical scanners, this is achieved by setting the phase cycling angle (ϕ_{cyc}) at 180° and by keeping the phase evolution angle ($2\cdot\pi\cdot\Delta f\cdot TR \approx 0$) close to zero with a short TR and with good shimming within the region of interest ($\Delta f \approx 0$). However, strong signals can also be observed when ϕ_{tot} is an integer multiple of 360° away from 180°, i.e., $\phi_{tot} \cong 180° + n\cdot 360°$ (n = 0, ± 1, ± 2, ...). In contrast, dark signals (i.e., dark banding artifacts) can be observed when ϕ_{tot} is an integer multiple of 360° away from 0°, i.e., $\phi_{tot} \cong n\cdot 360°$ (n = 0, ± 1, ± 2, ...). These high intensity and low intensity regions are called "pass band" and "transition band", respectively. Figure 3 shows the signal intensity as a function of the phase evolution angle ($2\cdot\pi\cdot\Delta f\cdot TR$) at four different phase cycling angles (ϕ_{cyc}) of 0°, 90°, 180°, and 270° and this function was simulated based on equations by Scheffler and Hennig (11). As shown in Figure 3, the bSSFP signal profile is periodic and the signal magnitude profile repeated every TR^{-1} Hz whereas the signal phase profile evolved every 2 TR^{-1} Hz. The location of the pass bands and transition bands shifted with the phase cycling angle (Fig. 3). The phase had only limited change in the pass band regions whereas steep phase changes were observable in the transition band regions. As mentioned above, the conventional bSSFP sequence, which is installed in most clinical scanners, corresponds to Figure 3C, where the on-resonance spins are in the middle of the pass band.

Recently, the bSSFP technique has been rediscovered in the context of imaging physiological and functional

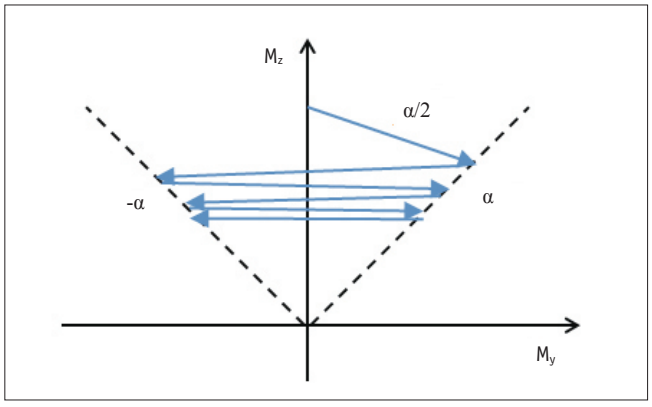

Fig. 2. Magnetization changes of balanced steady-state free precession (bSSFP) sequence with half-alpha preparation and phase-cycling angle of 180°. M_z denotes longitudinal magnetization and M_y denotes transverse magnetization along y-axis in rotating frame, and α denotes flip angle of radio frequency pulse. Notice that magnitude of transverse magnetization is maintained when bSSFP signal reaches steady-state.

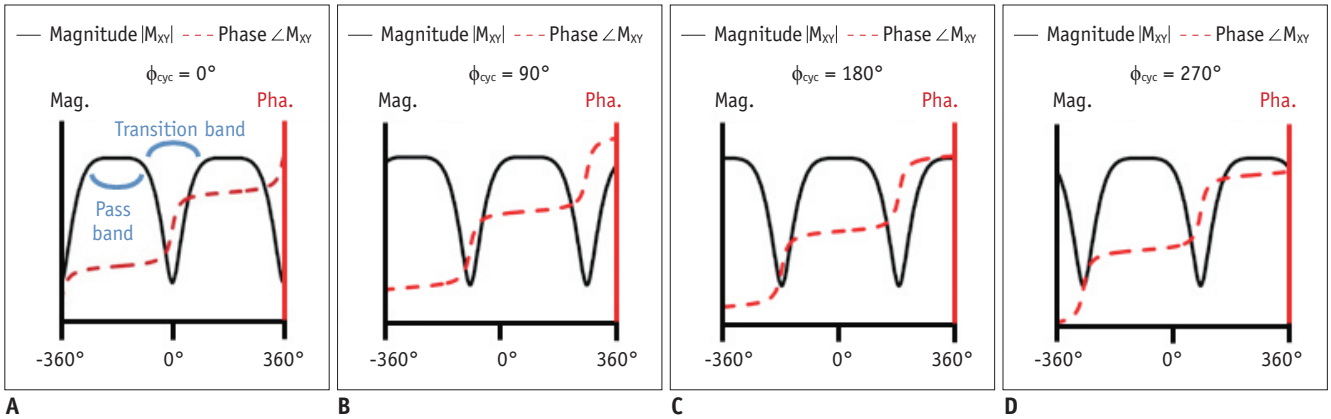

Fig. 3. Balanced steady-state signal profile as function of off-resonance frequency in one repetition time.
Magnitude and phase responses of balanced steady-state free precession (bSSFP) signals are shown as function of off-resonance precession angle per each repetition time. bSSFP signal profile for phase-cycling angles of 0° **(A)**, 90° **(B)**, 180° **(C)**, and 270° **(D)** are shown. Notice that signal profile is periodic and that signal profile shifts with each phase-cycling angle.

Korean Journal of Radiology
KJR

information. In contrast to its name, bSSFP for physiological MRI with no contrast agent should be performed in transient states of bSSFP acquisitions in order to sensitize the initial magnetization differences that are induced by a dedicated magnetization preparation module, such as arterial spin labeling (ASL), whereas the fMRI should be performed in the steady state due to the dynamic acquisition nature of fMRI. Because of its sensitivity to subtle changes in frequency and/or phase, high speed, high SNR, and no spatial distortion, bSSFP is a good candidate for physiological and functional MRIs.

Physiological Imaging

Magnetic resonance imaging is widely used to image the anatomy of blood vessels, especially for the evaluation of arteries and veins in clinical applications. Also, perfusion MR images are important for obtaining micro-vascular information. The bSSFP technique is potentially useful for imaging blood vessels in many aspects, mainly due to the unique contrast it can provide (i.e., T2/T1), which highlights blood signals from normal tissue (12). bSSFP shows less sensitivity to magnetic field inhomogeneity, unlike the conventional physiological techniques with EPI. Other benefits include the relatively high SNR and high spatial resolution, within a reasonable amount of time. Currently, bSSFP is commonly used for cardiac applications in clinical scanners, providing high signal intensity and blood/myocardium contrast (13). This review will main focus on the non-enhanced perfusion imaging using bSSFP.

The usefulness of the bSSFP readout for ASL with flow-sensitive alternating inversion recovery (FAIR) (14) was initially demonstrated in the body (kidney), where severe magnetic field inhomogeneity exists and high spatial resolution is required (15-17). Later, FAIR with a bSSFP readout was tried on the brain (18, 19), myocardium (20), muscle (21), and breast (22). In a similar context, the pseudo-continuous arterial spin labeling (pCASL) technique (23, 24) can be combined with a bSSFP readout for distortion-free high-resolution perfusion mapping. Exemplary three-dimensional pCASL-bSSFP images in the brain are shown in Figure 4. The pCASL-bSSFP combination has been applied for mapping perfusion in retina and kidney, regions where distortion and signal dropout effects are prominent with the conventional pCASL with EPI technique (25). In this work, banding and motion artifacts were reduced by employing a multiple phase-cycling approach (retina) and single breathe-hold (kidney), respectively. These ASL studies with a bSSFP readout have shown feasibility for non-invasive high resolution

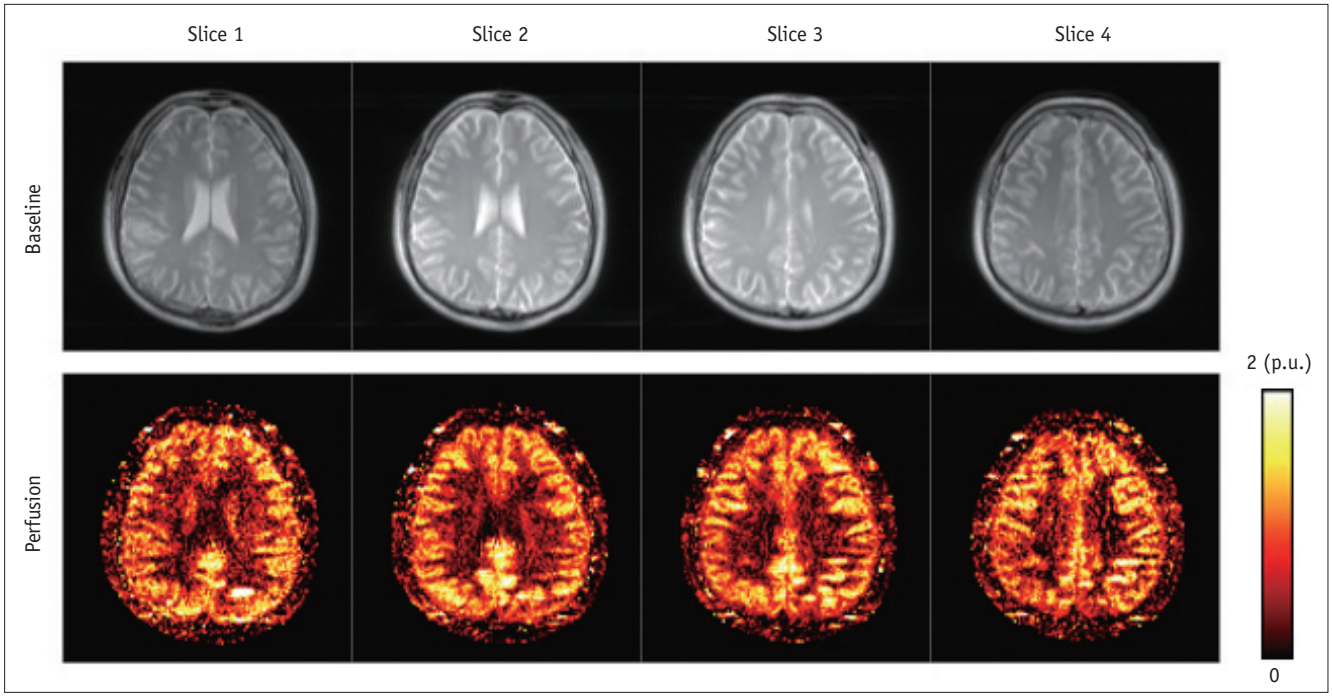

Fig. 4. Baseline and cerebral blood flow images of brain and were acquired using three-dimensional pseudo-continuous arterial spin labeling technique with balanced steady-state free precession readout scheme. Repetition time/echo time = 4/2 ms, field of view = 240 x 180 x 20 mm^3, matrix = 128 x 96 x 4, number of average for pair-wise subtraction = 40, and scan time = 4 minutes. p.u. = percent unit

mapping of blood flow in many different organs, possibly complementing the contrast agent techniques that especially useful for patients with kidney dysfunction.

The longitudinal magnetization of flowing blood was less affected by the bSSFP RF excitation pulse train than that of stationary tissues (26); however, it quickly recovered as T_1 decreased when blood perfused into the tissue. Recently, a few different studies were performed based on this phenomenon (27-29). In these studies, FAIR was combined with an ordinary bSSFP readout scheme or a segmented, multi-phase bSSFP readout scheme for non-enhanced MR angiography (27, 29) and the quantification of arterial cerebral blood volume (aCBV) (28). Although these techniques provided lower spatial resolution and coverage than the standard contrast-enhanced techniques, feasibility was shown for non-invasively imaging the cerebral vasculature and measuring aCBV in small vascular compartments (e.g., in small arteries, arterioles, and capillaries); this ability can be useful for clinical evaluation of cerebral perfusion.

A different approach has also been proposed for the simultaneous acquisition of both perfusion and magnetization transfer (MT) images, utilizing the inter-slice blood flow and magnetization transfer effects in two-dimensional multi-slice bSSFP imaging with no separate labeling pulse (30-32). This technique is termed alternate ascending/descending directional navigation (ALADDIN), where the perfusion signal was separated from the MT effects via different combinations of datasets with alternations in the multi-slice acquisition ordering and slice-select gradient polarity. The main advantage of this technique was in the labeling planes automatically tracking the imaging planes; this ability is proposed to be helpful for the detection of heterogeneous blood flow directions. Figure 5 shows exemplary directional perfusion maps obtained in the brain with a scan time of –3 minutes. Figure 6 shows the perfusion and MT asymmetry signals acquired with ALADDIN in cervical spines, where EPI suffers from significant susceptibility effects. The clinical usefulness of directional perfusion and MT asymmetry information needs to be investigated further.

In other studies, bSSFP have been developed for clinical evaluation of peripheral blood flow in combination with pre-saturation pulse, suppressing background tissue and venous signals while capturing the arterial inflow signal (33, 34). Although the quality was slightly lower than those with contrast-enhancement, the non-invasive nature and feasibility for diagnosis provided potential usefulness for clinical applications (33). Additional developments were made to quantify blood flow by combining bSSFP with phase contrast imaging technique, showing an accurate depiction of cerebral blood and cerebrospinal fluid flow (35).

Blood Oxygenation Level Dependent Functional MRI

When bSSFP is applied to fMRI, the functional signal changes can induce frequency shifts in 1) a pass band region, 2) a transition band with steep phase changes, or 3) a pass band of the opposite polarity (180° phase

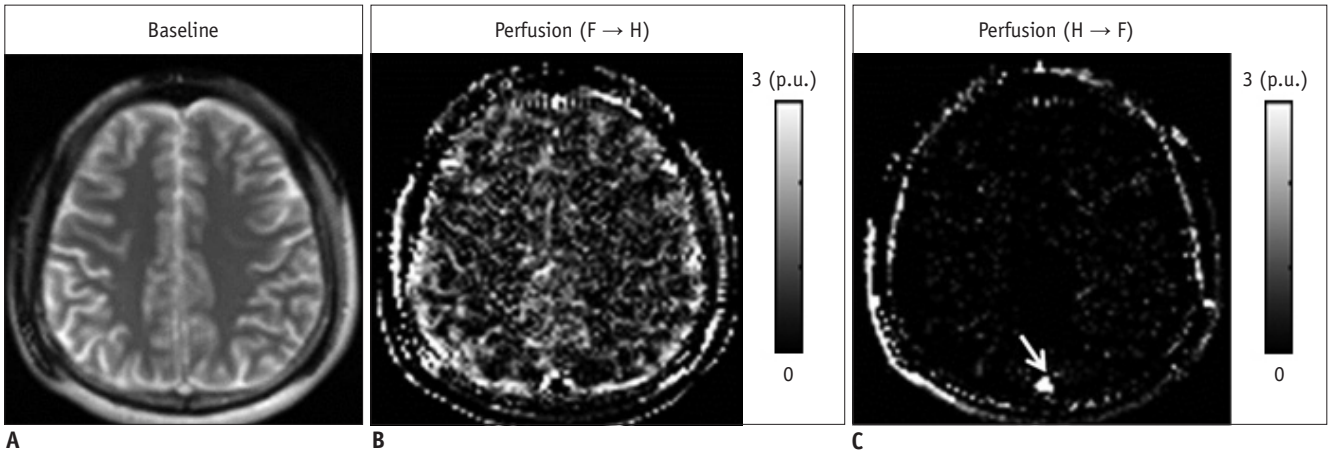

Fig. 5. Inter-slice blood flow images acquired with alternate ascending/descending directional navigation (ALADDIN).
Balanced steady-state free precession sequence is used for ALADDIN acquisition. Baseline **(A)**, perfusion with direction from feet (F) to head (H) **(B)**, and perfusion with direction from head (H) to feet (F) **(C)** images are shown. Arrow indicates superior sagittal sinus. Repetition time/echo time = 4/2 ms, field of view = 230 x 230 mm^2, matrix = 128 x 128, slice thickness = 5 mm, phase oversampling = 50%, number of slices = 15, number average for pair-wise subtraction = 8, and scan time = –3 minutes. p.u. = percent unit

Korean Journal of Radiology
KJR

difference), complicating the application of bSSFP to fMRI. Depending on the scan conditions (e.g., TR) and shimming conditions, bSSFP fMRI may depend on T2 or T2*, which have been shown to have different fMRI signal characteristics and, thus, make the interpretation of bSSFP fMRI signals complicated. Because of few phase changes in the pass bands (Fig. 3), the contrast of bSSFP is expected to be closer to T2 rather than T2* (exactly T2/T1). This fact is true when the imaging region is within a pass band. However, initial bSSFP fMRI studies have focused on improving the BOLD sensitivity by utilizing the transition bands (rather than pass bands) in expectation of the high phase sensitivity of the transition bands (Fig. 3) due to the frequency shifts induced by neuronal activity (36-41). Despite the high sensitivity to BOLD fMRI signals, the transition bands cover only narrow spatial regions and are sensitive to B_0 drift, limiting the application of this approach to fMRI. Some strategies, such as combination of multiple fMRI datasets acquired at multiple offset frequencies (37, 38, 41) and for minimizing B_0 drift effects such as real-time B_0 compensation (39, 41), were proposed for increasing the spatial coverage of transition-band bSSFP for fMRI.

Later, BOLD fMRI based on pass-band bSSFP was proposed and then became more popular for bSSFP fMRI (42-45). Pass-band bSSFP provided wider spatial coverage and more stable performance than the transition-band bSSFP for fMRI, but the signal sources in the pass-band bSSFP fMRI were not clear. The signal sources were considered to be T2* at long TR (44, 45), T2 at short TR (44), or diffusion in the extravascular area (46). The improvement of tissue specificity of that pass-band bSSFP fMRI that was based on T2 characteristics was demonstrated with computer simulations (47-49). The signal characteristics of bSSFP fMRI depended on the spatial location of the pass bands and transitions bands, which were not easy to assess with human fMRI because of the limitation in spatial resolution.

The heterogeneity in the signal sources of the pass-band bSSFP fMRI was experimentally investigated in high spatial resolution at a high field of 9.4-T (50). Figure 7 shows the rat forepaw fMRI studies with four different sequences of fast low angle shot (FLASH), transition-band bSSFP, pass-band bSSFP with TR = 10 ms, and pass-band bSSFP with TR = 20 ms, performed at 9.4-T, similar to but different from the study by Park et al. (50) in terms of better sensitivity (using a two-ring quadrature surface coil) and a better spatial resolution. The FLASH and transition-band bSSFP were sensitive to the phase changes and, thus, the activation foci were localized more on the draining veins, including the intracortical veins, as they can be assessed by comparison with the corresponding venogram (Fig. 7E) (51). The pass-band bSSFP also showed high fMRI signals but was less localized on the draining veins, implying T2 characteristics under this scan condition, whereas the long TR of 20 ms showed the localization of activation foci on draining veins, indicating T2* characteristics. When pass-band bSSFP with TR = 10 ms was used at multiple phase cycling angles of 0°, 90°, 180°, and 270° (50), the sensitivity and spatial specificity of fMRI maps changed with the phase cycling angle, indicating that the T2 or T2*

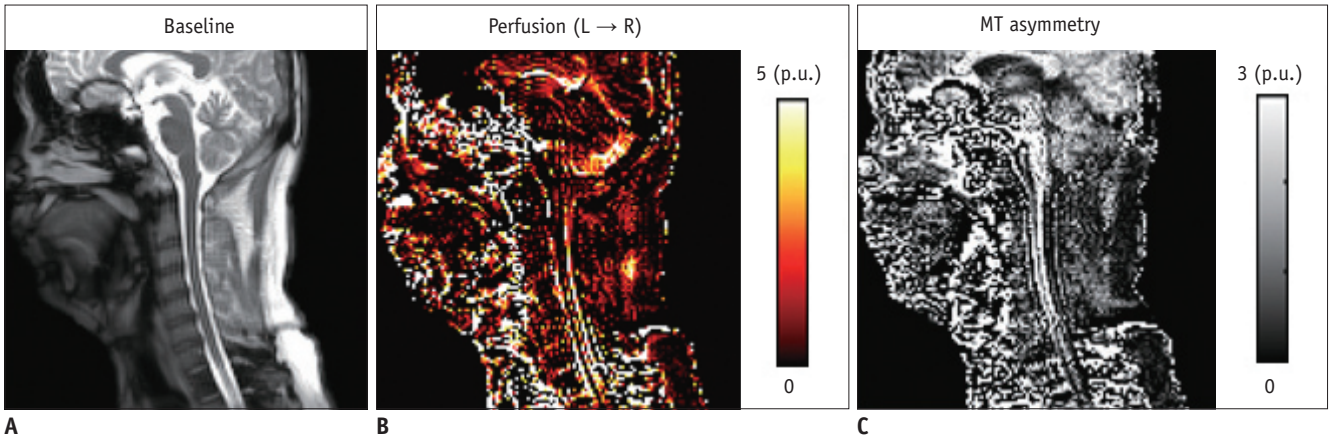

Fig. 6. Sagittal view of inter-slice blood flow and magnetization transfer (MT) asymmetry images in cervical spines simultaneously acquired with alternate ascending/descending directional navigation (ALADDIN).
Balanced steady-state free precession sequence is used for ALADDIN acquisition. Baseline **(A)**, perfusion **(B)**, and MT asymmetry **(C)** images are shown. Repetition time/echo time = 4/2 ms, field of view = 240 x 240 mm^2, matrix = 128 x 128, slice thickness = 4 mm, phase oversampling = 50%, number of slices = 13, number average for pair-wise subtraction = 8, and scan time = ~3 minutes. p.u. = percent unit

characteristics of pass-band bSSFP fMRI were dependent on the phase cycling angle and, thus, anatomical regions and structures associated with the shimming condition.

Most pass-band bSSFP fMRI studies have been performed with relatively long TR to weight T2* contrast for better sensitivity. Recently, resting-state fMRI was successfully performed with pass-band bSSFP with a short TR of 4 ms at 3 T and 2.5 ms at 7 T (52). The conventional bSSFP fMRI was also performed at TR of 3.8 ms at 7 T after an injection of monocrystalline iron oxide nanoparticle (53). These studies indicated that short-TR bSSFP might be applied for both conventional stimulation-based fMRI and resting-state fMRI but they require further assessment.

DISCUSSION

Many physiological and functional imaging methods can be incorporated using bSSFP as a data readout sequence, as mentioned above. bSSFP has high sensitivity to the initial magnetization difference, and, thus, it can be well combined with various magnetization preparation schemes for physiological MRI. Because of multiple RF excitations, the initial magnetization difference can decrease with RF excitation (7, 15, 25), and, thus, centric phase-encoding order is preferred over linear phase-encoding order for physiological MRI. While most physiological MRI methods require a separate magnetization preparation module, some unique bSSFP methods, such as ALADDIN, can provide relevant physiological information with no separate preparation module (30-32), making the time-efficient bSSFP sequence even more efficient. It is obvious that bSSFP can be combined with other physiological MRI methods that are not mentioned here and that new physiological imaging methods can be created in the future based on the unique characteristics of bSSFP.

Careful consideration is required for the usage of bSSFP for physiological and functional imagings. bSSFP suffers from transient oscillation and eddy current effects, especially, for centric phase-encoding order which is required for physiological MRI, and, thus methods, such as special pairing of consecutive phase-encoding lines, double averaging of single K-space line, or gradient waveform grouping, may be used to suppress these effects (54-56). Artifacts due to the transient signal oscillations may can also be reduced by using additional pre-pulses and pre-scans, such as half-alpha preparation or dummy phase-

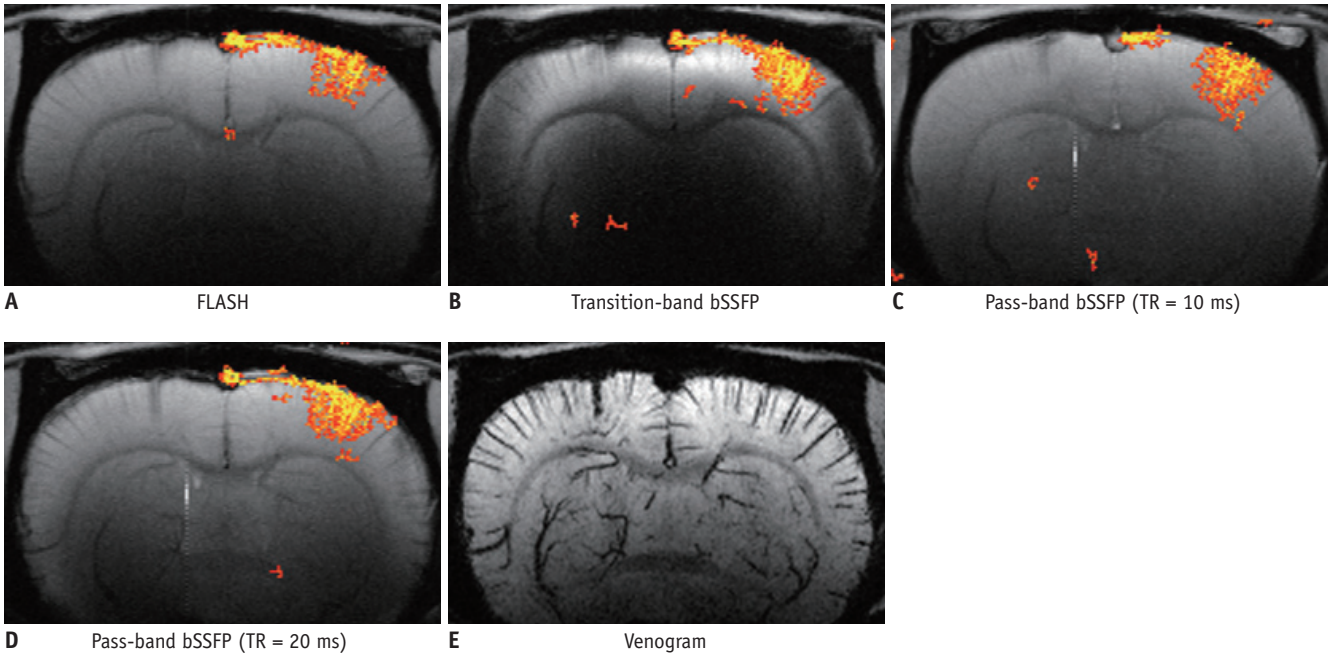

Fig. 7. Investigation of activation foci of high-resolution functional MRI maps.
Functional MRI maps acquired at 9.4-T with fast low angle shot (FLASH) **(A)**, transition-band balanced steady-state free precession (bSSFP) with time to repeat (TR) = 20 ms **(B)**, pass-band bSSFP with TR = 10 ms **(C)**, and pass-band bSSFP with TR = 20 ms **(D)**. Echo time was set to half of TR for all images. Each functional MRI map is overlaid on corresponding averaged baseline image. Matrix size = 256 x 128, field of view = 2.2 x 1.1 cm^2, slice thickness = 1 mm, and number of slice = 1 for all images. Flip angle was 8°, 4°, 16°, and 16° for images in **A-D**, respectively, and angles were optimized based on simulation at 9.4-T. **E.** Venogram with minimum intensity projection at same location as functional MRI maps in **A-D**.

Korean Journal of Radiology
KJR

encoding steps with linearly increasing flip angle.

One of the main drawbacks of bSSFP is banding artifacts in the regions of magnetic field inhomogeneity (transition regions in Fig. 3). Short TR and good shimming are strategies to suppress the artifact, as mentioned before. Special shim methods dedicated to bSSFP imaging may also be employed (57). The major advantage of these approaches is that no change in total scan time occurs, but the banding artifacts may not be perfectly removed. Another method is to combine the datasets that are acquired as multiple phase-cycling angles. Various methods for combining the multiple datasets have been proposed (58-60). This approach can virtually cover all cases of variations in the bSSFP profile (Fig. 3), however, at the cost of increased scan time. Other methods include reshaping the signal profile to broaden the range of the off-resonance precession angles (61) and dynamically phase-cycling with radial bSSFP imaging (62). These strategies will be helpful for suppressing the banding artifacts for physiological MRI and fMRI with bSSFP.

Although bSSFP is the fastest MRI method among the non-EPI sequences, its acquisition speed is still not as high as EPI, limiting the spatial coverage of physiological MRI and fMRI. Potential approaches to increasing the spatial coverage of bSSFP-based physiological MRI and fMRI would be a combination of bSSFP with acceleration algorithms, such as parallel imaging (63, 64) and compressed sensing (65-68). bSSFP utilizes each separate RF excitation per K-space line; this ability is favorable for the application of the acceleration algorithms. bSSFP-based fMRI has been demonstrated to be accelerated by parallel imaging (69) and compressed sensing (70). These technical advancements will allow for physiological MRI and fMRI that are free of distortion and the full coverage of the targeted organ in almost the same scan time as the conventional EPI-based imaging.

CONCLUSION

Balanced steady-state free precession is a promising technique for imaging physiological and functional information. The technique provides a unique signal profile and contrast, which can be helpful for various applications, with additional benefits of high SNR, high spatial resolution, and relatively high acquisition speed. Although the technique requires improvement for applications to physiological MRI and fMRI, feasibility is shown for clinical evaluation. Advancements can still be made with many possibilities, improving its usage in many clinical and neuroscience studies.

REFERENCES

1. Alsop DC. Phase insensitive preparation of single-shot RARE: application to diffusion imaging in humans. *Magn Reson Med* 1997;38:527-533
2. Feinberg DA, Kiefer B, Johnson G. GRASE improves spatial resolution in single shot imaging. *Magn Reson Med* 1995;33:529-533
3. Crelier GR, Hoge RD, Munger P, Pike GB. Perfusion-based functional magnetic resonance imaging with single-shot RARE and GRASE acquisitions. *Magn Reson Med* 1999;41:132-136
4. Carr HY. Steady-state free precession in nuclear magnetic resonance. *Phys Rev* 1958;112:1693-1701
5. Zur Y, Stokar S, Bendel P. An analysis of fast imaging sequences with steady-state transverse magnetization refocusing. *Magn Reson Med* 1988;6:175-193
6. Oppelt A, Graumann R, Barfuss H, Fischer H, Hartl W, Shajor W. FISP-a new fast MRI sequence. *Electromedica* 1986;54:15-18
7. Scheffler K, Lehnhardt S. Principles and applications of balanced SSFP techniques. *Eur Radiol* 2003;13:2409-2418
8. Miller KL. FMRI using balanced steady-state free precession (SSFP). *Neuroimage* 2012;62:713-719
9. Bieri O, Scheffler K. Fundamentals of balanced steady state free precession MRI. *J Magn Reson Imaging* 2013;38:2-11
10. Miller KL, Tijssen RHN, Stikov N, Okell TW. Steady-state MRI: methods for neuroimaging. *Imaging in Medicine* 2011;3:93-105
11. Scheffler K, Hennig J. Is TrueFISP a gradient-echo or a spin-echo sequence? *Magn Reson Med* 2003;49:395-397
12. Carr JC, Simonetti O, Bundy J, Li D, Pereles S, Finn JP. Cine MR angiography of the heart with segmented true fast imaging with steady-state precession. *Radiology* 2001;219:828-834
13. Hays AG, Schär M, Kelle S. Clinical applications for cardiovascular magnetic resonance imaging at 3 tesla. *Curr Cardiol Rev* 2009;5:237-242
14. Kim SG. Quantification of relative cerebral blood flow change by flow-sensitive alternating inversion recovery (FAIR) technique: application to functional mapping. *Magn Reson Med* 1995;34:293-301
15. Martirosian P, Klose U, Mader I, Schick F. FAIR true-FISP perfusion imaging of the kidneys. *Magn Reson Med* 2004;51:353-361
16. Boss A, Martirosian P, Graf H, Claussen CD, Schlemmer HP, Schick F. High resolution MR perfusion imaging of the kidneys at 3 Tesla without administration of contrast media. *Rofo* 2005;177:1625-1630
17. Fenchel M, Martirosian P, Langanke J, Giersch J, Miller S, Stauder NI, et al. Perfusion MR imaging with FAIR true

FISP spin labeling in patients with and without renal artery stenosis: initial experience. *Radiology* 2006;238:1013-1021
18. Boss A, Martirosian P, Klose U, Nägele T, Claussen CD, Schick F. FAIR-TrueFISP imaging of cerebral perfusion in areas of high magnetic susceptibility differences at 1.5 and 3 Tesla. *J Magn Reson Imaging* 2007;25:924-931
19. Ludescher B, Martirosian P, Klose U, Nägele T, Schick F, Ernemann U. Determination of the rCBF in the amygdala and rhinal cortex using a FAIR-TrueFISP sequence. *Korean J Radiol* 2011;12:554-558
20. Zun Z, Wong EC, Nayak KS. Assessment of myocardial blood flow (MBF) in humans using arterial spin labeling (ASL): feasibility and noise analysis. *Magn Reson Med* 2009;62:975-983
21. Boss A, Martirosian P, Claussen CD, Schick F. Quantitative ASL muscle perfusion imaging using a FAIR-TrueFISP technique at 3.0 T. *NMR Biomed* 2006;19:125-132
22. Buchbender S, Obenauer S, Mohrmann S, Martirosian P, Buchbender C, Miese FR, et al. Arterial spin labelling perfusion MRI of breast cancer using FAIR TrueFISP: initial results. *Clin Radiol* 2013;68:e123-e127
23. Dai W, Garcia D, de Bazelaire C, Alsop DC. Continuous flow-driven inversion for arterial spin labeling using pulsed radio frequency and gradient fields. *Magn Reson Med* 2008;60:1488-1497
24. Wu WC, Fernández-Seara M, Detre JA, Wehrli FW, Wang J. A theoretical and experimental investigation of the tagging efficiency of pseudocontinuous arterial spin labeling. *Magn Reson Med* 2007;58:1020-1027
25. Park SH, Wang DJ, Duong TQ. Balanced steady state free precession for arterial spin labeling MRI: initial experience for blood flow mapping in human brain, retina, and kidney. *Magn Reson Imaging* 2013;31:1044-1050
26. Wu WC, Jain V, Li C, Giannetta M, Hurt H, Wehrli FW, et al. In vivo venous blood T1 measurement using inversion recovery true-FISP in children and adults. *Magn Reson Med* 2010;64:1140-1147
27. Hori M, Shiraga N, Watanabe Y, Aoki S, Isono S, Yui M, et al. Time-resolved three-dimensional magnetic resonance digital subtraction angiography without contrast material in the brain: initial investigation. *J Magn Reson Imaging* 2009;30:214-218
28. Yan L, Li C, Kilroy E, Wehrli FW, Wang DJ. Quantification of arterial cerebral blood volume using multiphase-balanced SSFP-based ASL. *Magn Reson Med* 2012;68:130-139
29. Yan L, Wang S, Zhuo Y, Wolf RL, Stiefel MF, An J, et al. Unenhanced dynamic MR angiography: high spatial and temporal resolution by using true FISP-based spin tagging with alternating radiofrequency. *Radiology* 2010;256:270-279
30. Park SH, Duong TQ. Alternate ascending/descending directional navigation approach for imaging magnetization transfer asymmetry. *Magn Reson Med* 2011;65:1702-1710
31. Park SH, Duong TQ. Brain MR perfusion-weighted imaging with alternate ascending/descending directional navigation. *Magn Reson Med* 2011;65:1578-1591
32. Park SH, Zhao T, Kim JH, Boada FE, Bae KT. Suppression of effects of gradient imperfections on imaging with alternate ascending/descending directional navigation. *Magn Reson Med* 2012;68:1600-1606
33. Hodnett PA, Koktzoglou I, Davarpanah AH, Scanlon TG, Collins JD, Sheehan JJ, et al. Evaluation of peripheral arterial disease with nonenhanced quiescent-interval single-shot MR angiography. *Radiology* 2011;260:282-293
34. Edelman RR, Sheehan JJ, Dunkle E, Schindler N, Carr J, Koktzoglou I. Quiescent-interval single-shot unenhanced magnetic resonance angiography of peripheral vascular disease: technical considerations and clinical feasibility. *Magn Reson Med* 2010;63:951-958
35. Santini F, Wetzel SG, Bock J, Markl M, Scheffler K. Time-resolved three-dimensional (3D) phase-contrast (PC) balanced steady-state free precession (bSSFP). *Magn Reson Med* 2009;62:966-974
36. Scheffler K, Seifritz E, Bilecen D, Venkatesan R, Hennig J, Deimling M, et al. Detection of BOLD changes by means of a frequency-sensitive trueFISP technique: preliminary results. *NMR Biomed* 2001;14:490-496
37. Miller KL, Hargreaves BA, Lee J, Ress D, deCharms RC, Pauly JM. Functional brain imaging using a blood oxygenation sensitive steady state. *Magn Reson Med* 2003;50:675-683
38. Miller KL, Smith SM, Jezzard P, Pauly JM. High-resolution FMRI at 1.5T using balanced SSFP. *Magn Reson Med* 2006;55:161-170
39. Lee J, Santos JM, Conolly SM, Miller KL, Hargreaves BA, Pauly JM. Respiration-induced B0 field fluctuation compensation in balanced SSFP: real-time approach for transition-band SSFP fMRI. *Magn Reson Med* 2006;55:1197-1201
40. Lee J, Shahram M, Schwartzman A, Pauly JM. Complex data analysis in high-resolution SSFP fMRI. *Magn Reson Med* 2007;57:905-917
41. Wu ML, Wu PH, Huang TY, Shih YY, Chou MC, Liu HS, et al. Frequency stabilization using infinite impulse response filtering for SSFP fMRI at 3T. *Magn Reson Med* 2007;57:369-379
42. Bowen CV, Menon RS, Gati JS. High field balanced-SSFP fMRI: a BOLD technique with excellent tissue sensitivity and superior large vessel suppression. *Proc Intl Soc Mag Reson Med* 2005:119
43. Lee JH, Dumoulin SO, Saritas EU, Glover GH, Wandell BA, Nishimura DG, et al. Full-brain coverage and high-resolution imaging capabilities of passband b-SSFP fMRI at 3T. *Magn Reson Med* 2008;59:1099-1110
44. Miller KL, Smith SM, Jezzard P, Wiggins GC, Wiggins CJ. Signal and noise characteristics of SSFP FMRI: a comparison with GRE at multiple field strengths. *Neuroimage* 2007;37:1227-1236
45. Zhong K, Leupold J, Hennig J, Speck O. Systematic investigation of balanced steady-state free precession for functional MRI in the human visual cortex at 3 Tesla. *Magn Reson Med* 2007;57:67-73
46. Bowen C, Mason J, Menon R, Gati J. *High field balanced-SSFP*

fMRI: examining a diffusion contrast mechanism using varied flip-angles. Seattle: Proc 14th ISMRM, 2006:665
47. Miller KL, Jezzard P. Modeling SSFP functional MRI contrast in the brain. *Magn Reson Med* 2008;60:661-673
48. Kim TS, Lee J, Lee JH, Glover GH, Pauly JM. Analysis of the BOLD Characteristics in Pass-Band bSSFP fMRI. *Int J Imaging Syst Technol* 2012;22:23-32
49. Patterson S, Beyea S, Bowen C. *Quantification of the BOLD contrast mechanism, including its dynamic approach to steady state, for pass-band balanced-SSFP fMRI*. Toronto: Proc Intl Soc Mag Reson Med, 2008:2382
50. Park SH, Kim T, Wang P, Kim SG. Sensitivity and specificity of high-resolution balanced steady-state free precession fMRI at high field of 9.4T. *Neuroimage* 2011;58:168-176
51. Park SH, Masamoto K, Hendrich K, Kanno I, Kim SG. Imaging brain vasculature with BOLD microscopy: MR detection limits determined by in vivo two-photon microscopy. *Magn Reson Med* 2008;59:855-865
52. Cheng JS, Gao PP, Zhou IY, Chan RW, Chan Q, Mak HK, et al. Resting-state fMRI using passband balanced steady-state free precession. *PLoS One* 2014;9:e91075
53. Zhou IY, Cheung MM, Lau C, Chan KC, Wu EX. Balanced steady-state free precession fMRI with intravascular susceptibility contrast agent. *Magn Reson Med* 2012;68:65-73
54. Bieri O, Scheffler K. Flow compensation in balanced SSFP sequences. *Magn Reson Med* 2005;54:901-907
55. Markl M, Leupold J, Bieri O, Scheffler K, Hennig J. Double average parallel steady-state free precession imaging: optimized eddy current and transient oscillation compensation. *Magn Reson Med* 2005;54:965-974
56. Nielsen JF, Nayak KS. Interleaved balanced SSFP imaging: artifact reduction using gradient waveform grouping. *J Magn Reson Imaging* 2009;29:745-750
57. Lee J, Lustig M, Kim DH, Pauly JM. Improved shim method based on the minimization of the maximum off-resonance frequency for balanced steady-state free precession (bSSFP). *Magn Reson Med* 2009;61:1500-1506
58. Bangerter NK, Hargreaves BA, Vasanawala SS, Pauly JM, Gold GE, Nishimura DG. Analysis of multiple-acquisition SSFP. *Magn Reson Med* 2004;51:1038-1047
59. Elliott AM, Bernstein MA, Ward HA, Lane J, Witte RJ. Nonlinear averaging reconstruction method for phase-cycle SSFP. *Magn Reson Imaging* 2007;25:359-364
60. Cukur T, Lustig M, Nishimura DG. Multiple-profile homogeneous image combination: application to phase-cycled SSFP and multicoil imaging. *Magn Reson Med* 2008;60:732-738
61. Bieri O, Klarhofer M, Scheffler K. *Chimera steady state free precession (chimera SSFP)*. Hawaii: Proceedings of the 17th Scientific Meeting of International Society for Magnetic Resonance in Medicine, 2009:2767
62. Benkert T, Ehses P, Blaimer M, Jakob PM, Breuer FA. Dynamically phase-cycled radial balanced SSFP imaging for efficient banding removal. *Magn Reson Med* 2014 Jan 29 [Epub]. http://dx.doi.org/10.1002/mrm.25113
63. Griswold MA, Jakob PM, Heidemann RM, Nittka M, Jellus V, Wang J, et al. Generalized autocalibrating partially parallel acquisitions (GRAPPA). *Magn Reson Med* 2002;47:1202-1210
64. Pruessmann KP, Weiger M, Scheidegger MB, Boesiger P. SENSE: sensitivity encoding for fast MRI. *Magn Reson Med* 1999;42:952-962
65. Gamper U, Boesiger P, Kozerke S. Compressed sensing in dynamic MRI. *Magn Reson Med* 2008;59:365-373
66. Jung H, Sung K, Nayak KS, Kim EY, Ye JC. k-t FOCUSS: a general compressed sensing framework for high resolution dynamic MRI. *Magn Reson Med* 2009;61:103-116
67. Lustig M, Donoho D, Pauly JM. Sparse MRI: the application of compressed sensing for rapid MR imaging. *Magn Reson Med* 2007;58:1182-1195
68. Lustig M, Donoho DL, Santos JM, Pauly JM. Compressed sensing MRI. *IEEE Signal Processing Magazine* 2008;25:72-82
69. Chappell M, Håberg AK, Kristoffersen A. Balanced steady-state free precession with parallel imaging gives distortion-free fMRI with high temporal resolution. *Magn Reson Imaging* 2011;29:1-8
70. Han PK, Park SH, Kim SG, Ye JC. Compressed Sensing for fMRI: Feasibility Study on the Acceleration of Non-EPI fMRI at 9.4T. *Biomed Res Int* 2015 [Epub ahead of print]